LETTER OF INTENT

Hypernuclear Physics at DAΦNE.

M. Agnello[a], G.C. Bonazzola[b], E. Botta[b], T. Bressani[b], D. Calvo[b], P. Camerini[c], S. Costa[b], A. Donzella[e], F. D'Isep[b], A. Feliciello[b], A. Filippi[b], P. Gianotti[b], N. Grion[c], C. Guaraldo[d], F. Iazzi[a], A. Lanaro[d], E. Lodi Rizzini[e], V. Lucherini[d], S. Marcello[b], B. Minetti[a], E. Rossetto[b], R. Rui[c], A. Sharma[b] and L. Venturelli[e]

[a]Dipartimento di Fisica del Politecnico di Torino and Istituto Nazionale di Fisica Nucleare, Sezione di Torino, I-10125 Torino, Italy

[b]Dipartimento di Fisica Sperimentale dell'Università di Torino and Istituto Nazionale di Fisica Nucleare, Sezione di Torino, I-10125 Torino, Italy

[c]Dipartimento di Fisica, Università di Trieste and Istituto Nazionale di Fisica Nucleare, Sezione di Trieste, I-34127 Trieste, Italy

[d]Istituto Nazionale di Fisica Nucleare, Laboratori Nazionali di Frascati, I-00044 Frascati, Italy

[e]Dipartimento di Elettronica per l'Automazione, Università di Brescia and Istituto Nazionale di Fisica Nucleare, Sezione di Torino, I-25060 Brescia, Italy

Abstract. The low-energy, background free and tagged K^-s from the $\phi(1020)$ decay produced at the DAΦNE ϕ-factory in Frascati offer a unique opportunity for high resolution hypernuclei spectroscopy with K^- at rest. In this paper we outline the general problematic of this interesting field, expose the physics motivations that support our proposal and, finally, describe the techniques foreseen for precise measurements of the hypernuclear level energies and their decay modes. In this regard we investigated the performances of a magnetic spectrometer foreseen for one of the interaction region of the DAΦNE machine. Details on the detector characteristics as well as on its response to all the particles in the final state will be extensively discussed.

1. Introduction

The study of hypernuclei is important for several physics topics, and we will discuss shortly here, as example, three specific cases: the Λ-hypernuclei spectroscopy and its relevance to nuclear physics, the possible existence of Σ-hypernuclei and finally a test of the validity of the ΔI= 1/2 rule in weak interactions for the process $\Lambda+N \rightarrow N+N$ (non-mesonic decay of hypernuclei). From the nuclear physics point of view, it is worth re-emphasing that Λ-hypernuclei provide the best example of the validity of the single particle model without the difficulties linked to the Pauli exclusion principle and to the pairing interactions, as in ordinary nuclei. In nonstrange nuclei, the single-particle strength is broadly fragmented with excitation energy, and a deeply bound hole-state is essentially unobservable. In a Λ-hypernucleus, the distinguishable Λ may occupy any orbital and its rather weak core interaction leads to a well-defined, sharp set of states.

More interesting is the unique possibility offered by Λ-hypernuclei of testing a new approach to the description of nuclear matter. Following the success of some of the quark models in outlining many features of the baryon spectrum, it has been suggested that they could be even more appropriate for describing the short range region of the baryon-baryon interaction. Following this approach, the nucleus has to be represented as built up with quark bags. Due to confinement, the bags behave like baryons at relatively large distances (> 1 fm) and interact through boson exchange as in the conventional model. At shorter distances (< 1 fm), the bags may overlap and fuse to form larger bags of six (or nine) quarks, where the interaction is carried out by quark and gluon exchange.

An example of how hypernucler physics may give unique answers to this fundamental problem is shown by Fig.1. In the first row the baryon configuration for ^{4}He and $^5_\Lambda$He are reported. The baryons are assumed to be distinguishable, with the component quarks fully confined. In the second row the opposite hypothesis is assumed, i.e. that the quarks are fully deconfined, so that they occupy quark shell orbitals. For ^{4}He there is no substantial difference between the nucleon and quark description. For $^5_\Lambda$He , on the contrary, one can notice that the u- and d-quarks of the Λ cannot stay in the $s_{1/2}$ orbital, but in the $p_{3/2}$ one, whereas the s-quark may occupy the lowest energy state. In the baryon picture, all the 5 elementary constituents may occupy the $s_{1/2}$ orbital. Then, if there is a partial deconfinement of quarks in nuclei, this effect could manifest itself more clearly in hypernuclei. As a matter of fact, the binding energy of $^5_\Lambda$He in the ground state is slightly smaller than that expected with the baryon picture, but more data on many hypernuclei are necessary before drawing any conclusion.

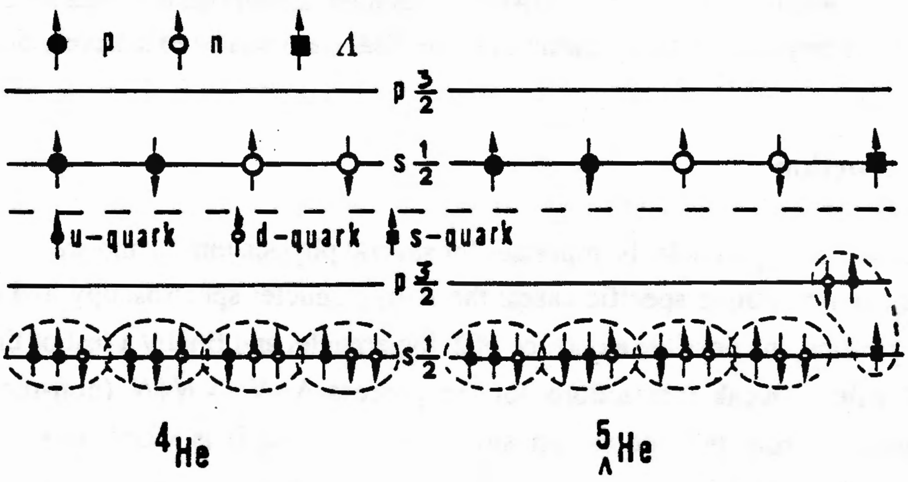

Fig. 1. Baryon (upper row) and quark (lower row) configurations for the ^{4}He and $^5_\Lambda$He systems.

A vigorous program of hypernuclear spectroscopy, providing precise measurements of the binding energy in the ground state and of the pattern of excited states would be essential in answering such questions.

The existence of Σ-hypernuclei is still a puzzle. The discovery of narrow peaks in production reactions, interpreted as due to defined Σ-hypernuclear states, was quite surprising. In fact, though the Σ-hyperon for many aspects is similar to the Λ-one, it was believed that its behaviour in nuclear matter was completely different. In fact, while Λ decay in nuclear matter proceeds through a weak interacting process ($\Delta S = 1$), Σ can decay through the strong interacting process ($\Delta S = 0$) $\Sigma + N \rightarrow \Lambda + N$. The width of the Σ-hypernuclear states are therefore expected to be a few tens of MeV. Following the first experiments at CERN and AGS which claimed the unexpected presence of narrow Σ-hypernuclear states, further detailed studies at KEK did not show evidence for the existence of Σ-hypernuclei, apart, perhaps $^{4}_{\Sigma}$He. A clear-cut answer to this intriguing puzzle is urgently needed. A recent review on the theoretical and experimental aspects of Σ-hypernuclei can be found in Ref.[1]

A free Λ-hyperon decays mostly into a nucleon and a pion via the weak non leptonic decay $\Lambda \rightarrow N + \pi$ with a lifetime of 2.63 10^{-10} s. The energy released in free decay is 37 MeV. Hypernuclei in their ground states also decay via weak interaction mechanisms. The situation, however, changes completely when the Λ is embedded in the nuclear medium. In the nucleus, the Λ is bound by up to 20 MeV (for heavy hypernuclei), so the phase space for the mesonic decay of the free Λ is greatly reduced. The final-state nucleon produced in the decay has a very low momentum (less than 100 MeV/c), and is consequently Pauli blocked. The result is an even further suppression of the hypernuclear mesonic decay mode. The nuclear medium affects the weak decay mode of the Λ hyperon by introducing a new non-mesonic decay mode. The corresponding energy release is approximately 176 MeV, leaving each of the final nucleons with a momentum of 417 MeV/c This decay mode has a much larger phase space (relative to the mesonic one) and the outgoing nucleons are not Pauli blocked, hence it dominates largely the weak decay process in medium or heavy hypernuclei. Very poor experimental data exist on the subject, however, due to the difficulty of producing hypernuclei and detecting the (n,p) and (n,n) pairs from the non-mesonic decays.

The most recent data from Brookhaven [2] seem to indicate, at a 2σ level, that the $\Delta I = 1/2$ rule, not theoretically understood, but assumed to hold for all weak decays and interactions, is no more valid for the non-mesonic decay of hypernuclei. In order to verify with a better statistical significance this possible violation, a measurement of the $\Lambda + n \rightarrow n + n$ and $\Lambda + p \rightarrow n + p$ relative branching ratios for several hypernuclei is necessary. More details on this argument can be found in the recent review paper of Cohen [3].

2. Production of hypernuclei

Neglecting for simplicity the hypernuclei production processes induced by antiprotons and relativistic ions, there are essentially two ways for producing and studying the hypernuclear spectra, with K^- beams and with π^+ beams.The larger amount of data has been produced so far by means of the strangeness exchange reaction:

$$K^- + n \rightarrow \Lambda + \pi^- \tag{1}$$

on a neutron of a nucleus, which transfers the strangeness from the K^- to the struck neutron, transforming it into a Λ. The reaction kinematics of (1) (Feshbach-Kerman kinematics) has the specific feature that, with the π^- detected at 0°, there is in the laboratory frame a "magic" value of the K^- momentum for which the Λ-hyperon is produced at rest, and the π^- carries all the momentum. The momentum transfer is then very small, 0 at the magic momentum (505 MeV/c), and can be varied in a controlled way by changing the beam momentum and/or the π^- emission angle. Hypernuclear final states for which the Λ has the same spin and orbital wave function of the transformed neutron are the most copiously ones produced in (1). The cross-sections may reach values of the order of mb/sr.

Recently, the associated production reaction :

$$\pi^+ + n \rightarrow K^+ + \Lambda \tag{2}$$

always on a neutron of a nucleus, was proved to be very efficient for producing Λ-hypernuclei at AGS. The kinematics of (2) is such that a relatively large momentum (~ 250 MeV/c) is transferred to the Λ-hyperon, always for forward detection of the K^+. The cross-sections are then lower by at least two orders of magnitude than those for (1), but this drawback is overcompensated by the larger intensities of the π^+ beams. The hypernuclear final states produced by (2) are different than for (1); mainly high spin hypernuclear states are observed.

A way of combining the advantages of (1) and (2): high production rate and many hypernuclear final states, is that of using reaction (1) but with K^- at rest. The momentum transferred to the produced Λ-hyperon is of the same order of magnitude (250 MeV/c) than (2) and the production rates for defined hypernuclear final states are still quite high: 10^{-3}/ stopped K^-. This technique was used very efficiently at KEK, when an impressive bulk of high quality data, with a lot of physics information was produced [4]. Fig. 2 shows a typical spectrum obtained at KEK with a ^{12}C target. The peaks are assigned as due to the ground state of ${}^{12}_{\Lambda}C$ and to the first excited state, of configurations $p^{-1}_{(3/2)n}s_\Lambda$ and $p^{-1}_{(3/2)n}p_\Lambda$ respectively.

It was noticed by Bressani [5] that K^- from ϕ decays could offer a unique opportunity for high-resolution hypernuclear spectroscopy.

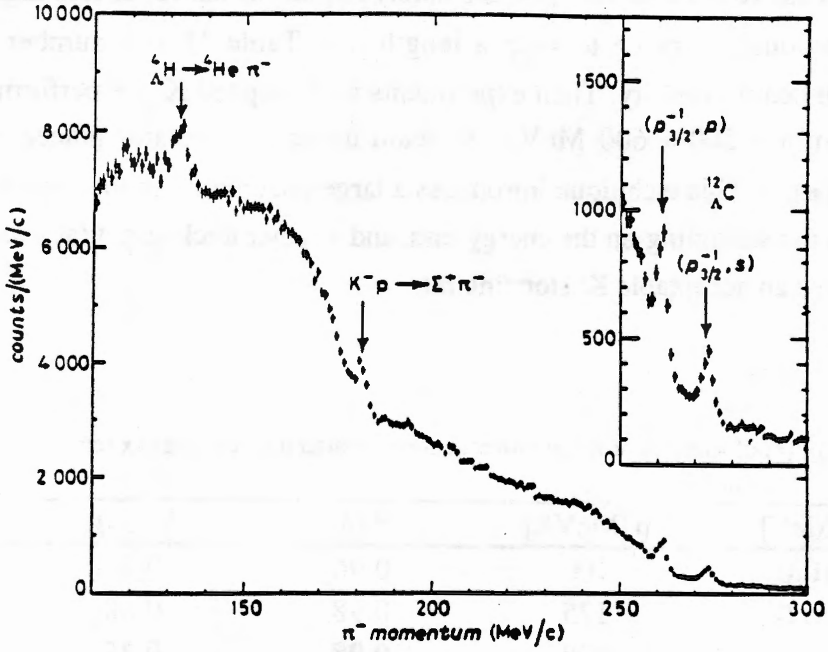

Fig. 2. π^- spectrum for $^{12}C(K^-_{stop}, \pi^-)$ reaction measured at KEK. The insert shows on an expanded scale the high momentum region, corresponding to the production of $^{12}_{\Lambda}C$ in the excited and ground state.

The arguments so far reported for Λ-hypernuclei are valid also for Σ-hypernuclei, mutatis mutandis in the kinematics due to the different mass of the Σ-hyperon. But the main problem is whether the Σ-hypernuclei exist at all !

More details on hypernuclear physics can be found in Ref.[6].

3. K⁻ at DAΦNE for hypernuclear spectroscopy

The total number of (K^+K^-) pairs from the φ-decay at $L = 10^{33} cm^{-2}s^{-1}$ will be ~ $2\ 10^3\ s^{-1}$. The source dimensions (the interaction region) will be negligible in the plane orthogonal to the colliding beams line (z-axis), of about 6 cm FWHM along z. Kaons will be emitted over 4π with an angular distribution proportional to $\sin^2\vartheta$, ϑ being the emission angle, measured relatively to the z-axis.

At first sight these features look quite discouraging when compared with those offered by K^- beams presently in operation at KEK and AGS, and even more at future machines (KAON). However, for some specific experiments, like high resolution hypernuclei spectroscopy with K^- at rest, DAΦNE might allow measurements which are substantially better than the present ones, and competitive also with those foreseen at KAON.

The reason stems from the low-energy (16.1 MeV) and cleanliness of the K^- from the ϕ-meson decay. At proton machines, where intense fluxes of kaons are emitted from a production external target, the distance between the source of particles and the experimental area is at least 10 ÷ 15 m, for radiation safety requirements. $K^{\pm}$ of less than 400 ÷ 450 MeV/c cannot obviously survive to such a length (see Table 1) in a number suitable to give a reasonable beam intensity. Then experiments with stopped K^- are performed by degrading in momentum a ~ 500 ÷ 600 MeV/c K^- beam using a moderator placed just in front of the stopping target. This technique introduces a large uncertainty in the momenta of the degraded K^-s due to the straggling on the energy loss, and a rather thick target (at least 1 g/cm^2) has to be used to have an acceptable K^- stopping rate.

Table 1

Probabilities P(x) of survival of $K^{\pm}$ at different energies after a given length x (cm).

T [MeV]	p [MeV/c]	P (3)	P (50)	P (100)
10.0	100	0.96	0.51	0.26
30.0	175	0.98	0.68	0.47
50.0	228	0.98	0.75	0.56
100.0	330	0.99	0.82	0.67

Apart the case of active targets, the uncertainty in the localization of the stopping point introduces an error on the determination of the emitted charged particles [π^- from the formation reaction

$$K^-_{stop} + {}^{A}X_Z \rightarrow {}^{A}_{\Lambda}X_Z + \pi^- , \qquad (3)$$

π^- from the hypernuclear states mesonic decay, p from the non-mesonic decay] which often degrades considerably the designed performances of the magnetic spectrometer.

On the contrary, the 16.1 MeV K^- produced at DAΦNE have a range of 1 g/cm^2 at maximum (depending on the material) and the straggling on the range is less than 50 mg/cm^2 (FWHM). The uncertainty on the interaction point leads typically to a momentum spread, for the outgoing pions, of the order of 100 KeV/c.

The 4π solid angle over which the kaons are emitted from the interaction region imposes some care on the target design and assembly. The interaction / target region, as proposed, is sketched in Figure 3. It consists of four concentric cylindrical regions: the inner beam pipe (with radius of 5 cm), a first cylindrical barrel of scintillators, the stopping target surrounded by an outer array (4 to 6 layers) of Si microstrips. The length of the cylinders will be of about 8 cm. The beam pipe must be kept as thin as possible, compatibly with the safety requirements. A thin Be pipe would be the most appropriate. The barrel of scintillators, viewed at both ends by fast photomultipliers will provide the selection of K^- by ΔE/Δx, at the first level trigger. The thickness of the stopping target must be such to allow the stopping of K^-s emitted from 45° to

135° with respect to the z-axis. More than 80% of the produced K^-s are expected to stop in the target. Tagging of the K^+, emitted collinear to the K^- ($\phi \rightarrow K^+K^-$) and with the same energy, will allow the determination of the interaction point within the target thickness.

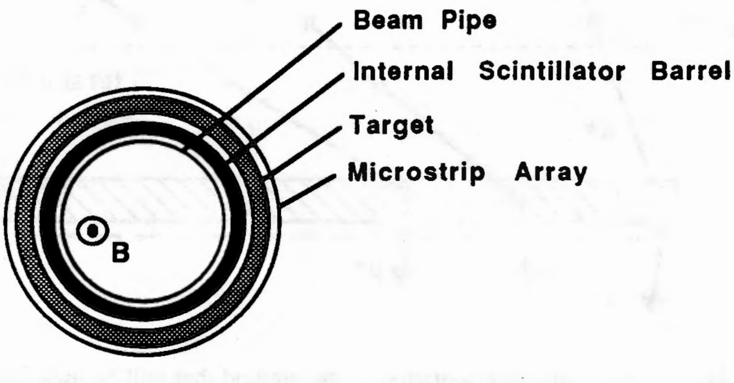

Fig. 3. Sketch of the interaction / target region (front cut view).

Once the K^+ and K^- are brought to rest, the K^+ will decay with its typical lifetime of 12.37 ns. The most frequent decay ($K_{\mu 2}$, 63.5%) will give a μ^+ of 236 MeV/c, emitted isotropically. The K^- instead will be captured in an external orbit, will cascade to the inner orbits and then interact with the capturing target nucleus. The capture rate for the production of well defined hypernuclear states, in two-body reaction of type (3), is of the order of 10^{-3}/stopped K^-; from the reaction a fast π^- (~ 250 ÷ 280 MeV/c) will be emitted isotropically. Both μ^+ and π^-, crossing the outside target boundaries, will be detected by the microstrip array placed in close contact with the target. Such an arrangement will give, with good precision, the position of both the decay (K^+) and interaction (K^-) points on the surface of the cylindrical target (see Figure 4).

In this way the angle ϑ of emission of the (K^+K^-) pair can be determined. Since the energy of kaons from ϕ decays is known precisely , the depth in the target at which the (K^-_{stop}, π^-) reaction occurs can be determined, and used furthermore for the necessary off-line corrections.

The information from microstrip detector will be also used for the determination of the momenta of the particles in the magnetic field. Furthermore, we suggest for it a layered structure in order to detect Λ's by means of their charged decay (π^- p).The detection of Λ's is very important in connection with the studies on Σ-hypernuclei production. As pointed out by Yamazaki [7] the method of the Λ detection is very powerful to suppress backgrounds from other physical processes (Σ^- decay, quasi-free Λ and Σ production, ...).

The above described design of interaction / target region imposes some limitations on the nuclear targets that can be used. Metals and solid materials are easily machined to such a shape, whereas it is very difficult to put into operation gaseous targets.

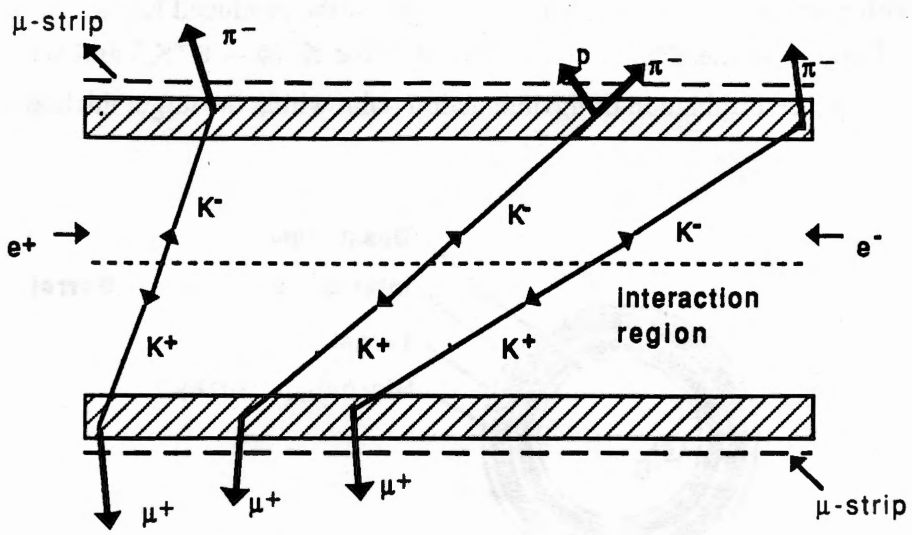

Fig. 4. Schematic representation of the method that will be used for reconstructing the interaction vertex inside the stopping nuclear target.

4. A Magnetic Spectrometer for hypernuclear spectroscopy at DAΦNE

The main features of a magnetic spectrometer capable of exploiting at best the unique properties of K^- interactions at DAΦNE are the following:

1) cylindrical geometry

2) large solid angle (> 2π)

3) excellent momentum resolution (~ 0.2% at ~ 270 MeV/c)

4) large momentum acceptance (100 ÷ 300 MeV/c)

5) possibility of detecting secondary slower charged particles (π and p from the decay of the hypernuclear levels).

Furthemore the apparatus should be able to detect neutrons from non-mesonic decays.

We have concentrated our efforts, up to the moment, on the optimization of the momentum resolution, which is the figure of merit for hypernuclear spectroscopy and which represents the most difficult task when considering non-focussing spectrometers. In a nearly homogeneous solenoidal field the minimal information necessary to determine the momentum of a charged particle is given by the coordinates of three points in the space along its trajectory. The first point, close to the target, is measured with a very good precision by means of the microstrip array. Further two points, at least, have to be measured by other devices.

Figure 5 is a layout of the proposed detector. It consists of a solenoid with a radius of ~ 1 m and a length of ~ 2 m, with a maximum field intensity of 1.5 T at the center. Three layers of detectors, all of cylindrical shape, are located inside the magnetic volume. At a radius of ~ 0.5 m there is a cylindrical (or polygonal) drift chamber, thin-walled, with ~ 150 drift wires parallel to the field lines, spaced by ~ 1 cm. The left-right ambiguity will be solved thanks to the method of the two adjacent sense wires. The designed resolution on the x-y plane will be

~ 150 μm FWHM. A less accurate determination of the z-coordinate can be obtained by the charge-division method. The total thickness of the materials of the chambers, particularly the mylar windows, must be minimized since it is the main source of multiple Coulomb scattering along the particle's trajectory, and affects directly the momentum resolution in such non-focussing spectrometers.

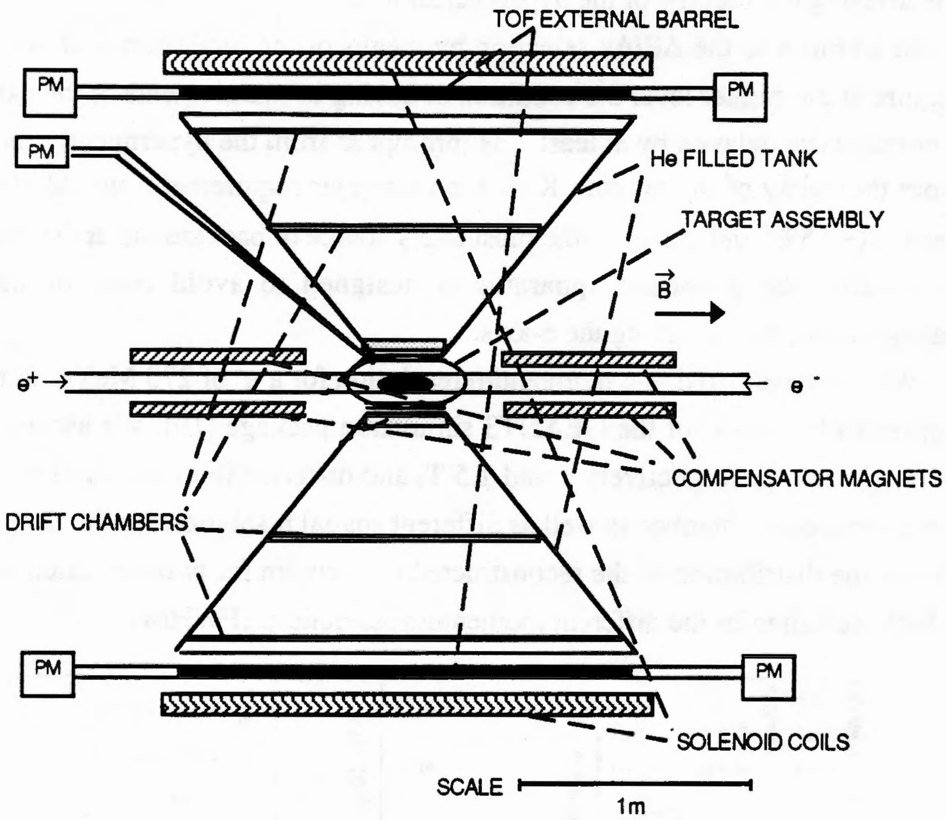

Fig. 5. Layout of the proposed magnetic spectrometer for (K^-_{stop}, π^-) reactions.

At a radius of ~ 1 m there is a set of two drift chambers that will provide the localization of the particle's impact point with a precision of ~ 150 μm FWMH in all directions. About 350 drift wires, with a wire spacing of 2 cm would be needed to this purpose, but there are no particular requirements on the total thickness of this chamber array due to its location at the end of particle's trajectories, inside the magnetic volume. All the chamber will be filled with the usual (Ar, C_2H_6) gas mixture.

All the drift chambers must be contained in a tank filled with Helium, at atmospheric pressure, to minimize the multiple Coulomb scattering. Due to the particular shape of the Helium tank which encloses the apparatus, the central small solenoids necessary to compensate the main solenoidal field could be located rather close to the interaction region.

The outermost detector consists of a second cylindrical barrel of scintillators (~ 80 elements, 200×8×10 cm^3 each) viewed at both ends by fast photomultipliers. It will allow Time-Of-Flight (T.O.F.) measurements, provide the first level trigger and detect neutrons from non-mesonic decays. The technique of compensation of the time spread in long scintillators with point-like source geometry [8] could be very useful for achieving a total time resolution of 1 ns FWHM at the trigger level. The relative alignment of all scintillator slabs will be done by means of an optical fibers / Laser set-up [9]. A total time resolution of 300 ps FWHM could be achieved in the final analysis, by means of various software corrections, and could possibly be exploited for studying the lifetime of the hypernuclear levels.

In addition to the $\Delta E/\Delta x$ selection by means of the inner barrel of scintillators, we could require at the trigger level the condition of having in two elements of the external T.O.F. barrel a coincidence delayed by at least 3 ns (prompt π^- from the hypernuclei production, delayed μ^+ from the decay of the tagging K^+). Such a trigger requirement would eliminate the $\phi \neq K\overline{K}$ decays (~ 15%) and therefore the most likely source of background at the trigger level.

Finally, the proposed apparatus is designed to avoid most of the electromagnetic backgrounds, peaked along the z-axis.

We have estimated the momentum resolution for a π^- of 270 MeV/c in the above described apparatus by means of the GEANT3 simulation package [10]. We assumed, for simplicity, a uniform field of respectively 1 and 1.5 T, and different thicknesses of the mylar windows of the central drift chamber as well as different spatial resolution for the drift chambers. Figure 5 shows the distribution of the reconstructed momentum for two simulated configurations, from which we can infer the different momentum resolutions (FWHM).

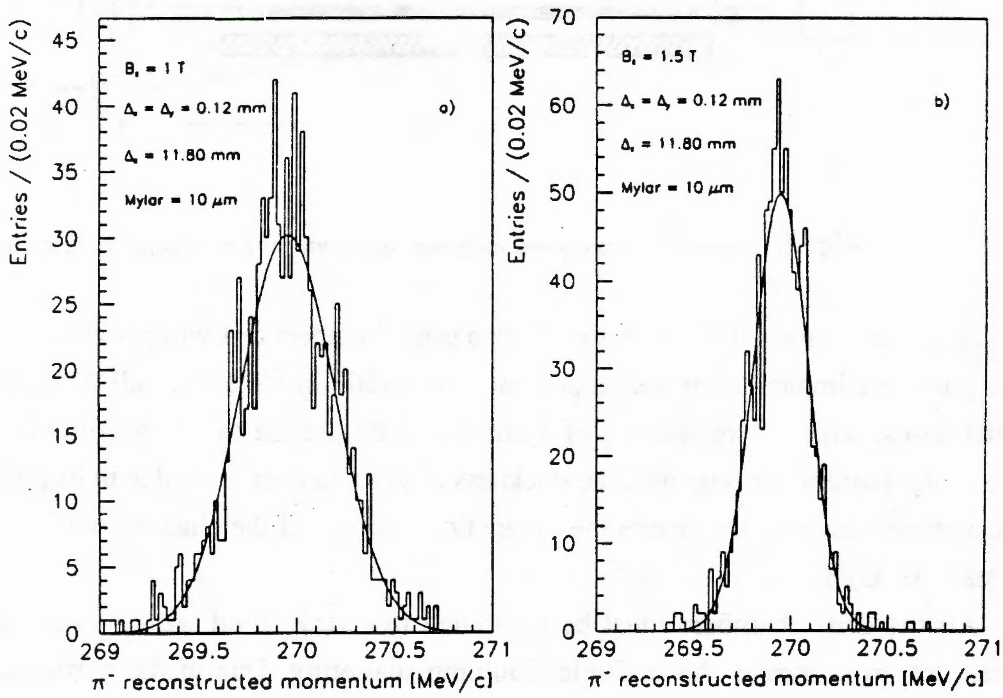

Fig. 6. Histograms of the reconstructed momenta distribution from Monte Carlo simulation. Monoenergetic π^- of 270 MeV/c, isotropically emitted from the center of the spectrometer were tracked in the apparatus by means of the GEANT3 package. The distribution has been obtained for the cases of a magnetic field intensity of, respectively, 1.0 T (a) and 1.5 T (b), a thickness of the mylar window of 10 μm and a nominal spatial resolution (FWHM) $\Delta x = \Delta y = 0.12$ mm, $\Delta z = 11.8$ mm for the drift chambers.

Table 2 summarizes the results of the simulations for all different cases. We may infer, from the momentum spectrum of the outgoing pions, that an energy resolution of less than 300 KeV on the measurements of the hypernuclear energy levels can be achieved in the most favourable cases.

Table 2

FWHM resolution for π^- of 270 MeV/c obtained with the apparatus sketched in Figure 4 (microstrips array at the beginning of the trajectories, one drift chamber in the middle, one drift chamber at the end) for different values of B, different values of the thickness of the mylar windows and of the drift chambers spatial resolution (FWHM).

magnetic field [T]	mylar window thickness [μm]	$\Delta x = \Delta y = 0$ mm $\Delta z = 0$ mm	$\Delta x = \Delta y = 0.12$ mm $\Delta z = 11.8$ mm	$\Delta x = \Delta y = 4.72$ mm $\Delta z = 47.2$ mm
1.0	10	1.79 ‰	2.10 ‰	4.30 ‰
1.0	20	2.31 ‰	2.41 ‰	4.34 ‰
1.0	30	2.62 ‰	2.76 ‰	---
1.5	10	1.20 ‰	1.23 ‰	2.50 ‰
1.5	20	1.27 ‰	1.42 ‰	2.71 ‰
1.5	30	1.63 ‰	1.84 ‰	---

However, such a simplified geometry, which optimizes the momentum resolution, is unfavourable for pattern recognition purposes and shows its limits particularly in the case when other charged particles, emitted in coincidence with the prompt pions, have to be detected. For this reason we simulated the response of a spectrometer with the same characteristics of the previous one, but with two thin-walled drift chambers, of radii 0.33 and 0.66 cm, respectively. Results are summarized in Table 3. A worsening of the momentum resolution on the outgoing pions is evident, but at a tolerable level.

Table 3

Same than Table 2, but with two thin drift chambers.

magnetic field [T]	mylar window thickness [μm]	$\Delta x = \Delta y = 0$ mm $\Delta z = 0$ mm	$\Delta x = \Delta y = 0.12$ mm $\Delta z = 11.8$ mm	$\Delta x = \Delta y = 4.72$ mm $\Delta z = 47.2$ mm
1.0	10	2.03 ‰	2.55 ‰	10.10 ‰
1.0	20	---	2.97 ‰	---
1.0	30	---	3.33 ‰	---
1.5	10	1.35 ‰	1.58 ‰	7.46 ‰
1.5	20	---	1.82 ‰	---
1.5	30	---	2.02 ‰	---

The best solution for an improved pattern recognition on the charged tracks could be obtained by using a Time Projection Chamber (TPC). However, the filling gas typically adopted (a mixture containing mostly Neon) contributes largely to the Coulomb multiple scattering. Nevertheless a Monte Carlo simulation of a TPC based apparatus is currently in progress.

With the proposed apparatus we expect a reasonable hypernuclei event rate. For $\mathcal{L} = 10^{32} cm^{-2} s^{-1}$, a target solid angle for stopping the K^- of 2π sr [corresponding to ~ 80% of the total (K^-K^+) production rate from ϕ decay], a solid angle for detecting the outgoing π^- of ~ π sr, a detection efficiency of ~ 0.5 (drift chambers + trigger + reconstruction), we estimated ~ 50 ev/hour for a single hypernuclear final state produced at a rate of 10^{-3}/stopped K^-, without tagging the event with the K^+. Tagging with the K^+ lowers the event rate to ~ 20 ev/hour. On the other hand, a capture rate of 10^{-3}/stopped K^- is the present limit of measurements at KEK reached on a single final state. Many final states may obviously be populated at the same time.

The large solid angle subtended by the spectrometer offers the unique possibility of measuring in coincidence the products from the decay of the hypernuclear levels. The external barrel of scintillators will allow detection of neutrons, with an efficiency of ~ 10%. We expect a total efficiency ($\Delta\Omega\times\varepsilon$) of ~ 30% for detection of mesonic decays (though physically strongly suppressed for medium-heavy hypernuclei), ~6% for $\Lambda + p \rightarrow n + p$ and 1% for $\Lambda + n \rightarrow n + n$ non-mesonic weak interactions of the Λ embedded in nuclear matter. We recall that information on the non-mesonic decays is very poor, in spite of its intrinsic interest, due to the experimental difficulties . Significative measurements on non-mesonic decays could be performed even at $\mathcal{L} = 10^{32} cm^{-2} s^{-1}$.

4. The status of the FINUDA experiment (Hypernuclei at DAΦNE)

The idea of using the K^- at DAΦNE for hypernuclear physics was put forward in 1990 at the INFN Directorate by T. Bressani, and was further discussed at the Folgaria School (February '91) and at the DAΦNE Workshop (April '91). In this occasion interest for participating to the experiment was expressed by groups from INS (Tokyo) and Dubna. Further interest in participation was expressed in July '91, during the NAN Workshop in ITEP (Moscow), by groups from Czechoslovakia (Bratislava and Prague).

A preliminary request of financial support to the experiment was put forward at the Nuclear Physics Committee (Gr. III) of INFN in July '91, for prototype studies.

It was satisfied (~ 80 ML).

During Fall '91 simulations of the apparatus, based on GEANT 3 package, were started and the program is now nearly completed.

The ideas concerning the physics and the apparatus were presented at the International Symposium on Hypernuclear and Strange Particle Physics, held in Shimoda (Japan) from 9 to

12 December 1991, and at the Comité d'Expériences in Saclay the 17 December 1991. Interest in participating to the experiment was manifested by groups of KAON (Vancouver) and Yerevan (Armenia). The Group of Trieste joined the collaboration in January 1992. F. Sauli from PPE (CERN) and A. Sharma expressed their interest in the development of the chambers for the spectrometer.

The experiment on hypernuclei at DAΦNE (FINUDA) was furthermore presented at the Nuclear Physics Committee (Gr. III) of INFN in February '92, as one of the major initiatives for the Five-Years Financial Plan 1994-1999.

At present, we envisage to prepare a Workshop on Hypernuclear and Low Energy Kaon Physics at DAΦNE in June1992, in order to define the duties of the different Groups of the Collaboration.

5. REFERENCES

1 C.B. Dover, D.J. Millener and A. Gal, *Phys. Rep.* **184** (1989), 1.
2 J.J. Szymonski et al., *Phys. Rev.* **C43** (1991), 849.
3 J. Cohen, in *Progress in Particle and Nuclear Phisics* Vol. **25** (1990), 139.
4 T. Yamazaki et al., *Nuovo Cimento* **102A** (1989), 695.
5 T. Bressani, Proc. Workshop on Physics and Detectors for DAΦNE, Frascati, April 9-12, 1991 (ed. G. Pancheri, Servizio Documentazione dei Lab. Naz. di Frascati, 1991), p. 475.
6 T. Bressani, in *Hadronic Physics at Intermediate Energy* Vol. I (North-Holland, Amsterdam, 1986), p.259
7 T. Yamazaki, Proc. Workshop on Physics and Detectors for DAΦNE, Frascati, April 9-12, 1991 (ed. G. Pancheri, Servizio Documentazione dei Lab. Naz. di Frascati, 1991), p. 315.
8 G.C. Bonazzola et al., IEEE Trans. Nucl. Science Vol. 36 (1989), 806.
9 G.C. Bonazzola et al., IEEE Trans. Nucl. Science Vol. 38 (1991), 393.
10 R. Brun et al., GEANT3 Data Handling Division DD/EE/84-1, September 1987.